Bathke, H., Shirzaei, M., Walter, T. R. (2011): Inflation and deflation at the steep-sided Llaima stratovolcano (Chile) detected by using InSAR. - Geophysical Research Letters, 38, L10304

DOI: 10.1029/2011GL047168

Inflation and deflation at the steep-sided Llaima stratovolcano (Chile) detected by using InSAR

H. Bathke,[1] M. Shirzaei,[1,2] and T. R. Walter[1]

Received 16 February 2011; revised 1 April 2011; accepted 1 April 2011; published 19 May 2011.

[1] Llaima volcano, Chile, is a typical basaltic-to-andesitic stratovolcano in the southcentral Andes. Llaima had at least four explosive eruptions in the decade 2000 – 2010, however little is known about the physical processes and magma storage at this volcano. In this study we present an InSAR deformation field at Llaima from 2003 – 2008, covering both the post-eruptive and syn-eruptive periods. The satellite InSAR data are significantly affected by environmental decorrelation due to steep topography, snow and vegetation; because of this, we applied a model-assisted phase unwrapping approach. The analysis of these data suggests two main deformation episodes: subsidence associated with the post-eruptive period, and uplift associated with the syn-eruptive period. Maximum summit subsidence and uplift are ~10 cm and ~8 cm, respectively. Through inverse modeling of both periods, a deflating and inflating magma body can be inferred, located at a depth of 4 – 12 km, subject to a volume decrease of $10 – 46 \times 10^6$ m^3 during the subsidence period, followed by a volume increase of $6 – 20 \times 10^6$ m^3 during the uplift period. Therefore, this study presents the first evidence of magma-driven deformation at Llaima volcano, and suggests that eruption periods are associated with the inflation and deflation of a deep magma body that can be monitored by using space geodesy. **Citation:** Bathke, H., M. Shirzaei, and T. R. Walter (2011), Inflation and deflation at the steep-sided Llaima stratovolcano (Chile) detected by using InSAR, *Geophys. Res. Lett.*, *38*, L10304, doi:10.1029/2011GL047168.

1. Introduction

[2] Llaima is one of the largest and most active volcanoes in the southern volcanic zone of South America, being a Holocene steep basaltic-to-andesitic stratocone with an edifice height of 3125 m and a volume of about 400 km^3 [*Naranjo and Moreno*, 1991]. The eruptive history of the volcano is of mainly Strombolian and Hawaiian type, however, intermittent sub-plinian activity poses a high hazard potential, including pyroclastic flows, air-falls and remobilization of material in the form of lahars [*Naranjo and Moreno*, 1991].

[3] Recent eruptions have occurred in 2002 and 2003, followed by a 4-year period of silence, and further eruptions again throughout 2007–2009; each eruptive period had individual phases of activity and quiescence [*Siebert and Simkin*, 2002]. There is a high probability of another imminent eruption [*Dzierma and Wehrmann*, 2010]. As there is only minor vulnerability in the poorly populated and hardly accessible region, only sparse monitoring networks have been installed until recently [*Galle et al.*, 2010]. Therefore, although being so prominent and well known volcanically, the physical processes of the magma supply at Llaima and its plumbing system are poorly understood. No magma chamber has been constrained so far, which would allow design and adjustment of monitoring networks.

[4] As we show herein, satellite data could provide one of the most important information sources. The space-borne synthetic aperture radar (SAR) technique is one of the few methods that enables us to look back in time and study deformation occurrence at Llaima volcano. Using interferometric SAR data, *Fournier et al.* [2010] identified a slow landslide at the eastern flank of Llaima. Association of the observed eruptions with deformation activity was not detected however, mainly because of temporal and spatial radar signal decorrelation.

[5] In this study we analyze a set of InSAR data and apply a model-assisted phase unwrapping and modeling approach to characterize the source of the deformation field based on noisy interferometric data sets. This approach allows us to identify two periods of activity: subsidence between 11/2003 and 05/2007 and uplift from 05/2007 until 11/2008. These periods of observation were preceded by a volcanic crisis on 04/16/2003 and included two other episodes of volcanic activity starting on 05/26/2007 and 01/01/2008 (Figure 1). Through inverse modeling of the observed deformation data we constrained the magmatic source geometry and strength underneath the volcano. This provided the first evidence of magma-driven deformation at Llaima volcano prior to, and after, volcanic crises.

2. Remote Sensing Data Set

[6] We firstly considered Landsat data to obtain a general overview of the study area. Figure 2 shows a Landsat TM image acquired in 1987, represented in band 432 false color. The color red in the image indicates vegetation, white shows snow and dark grey indicates exposed rocky surfaces. The snow-capped summit and the vegetated apron are clearly visible. In comparison with geologic lithologies [*Naranjo and Moreno*, 1991], the greyish colors in the Landsat image correlate with mainly historical lahars and pyroclastic flow deposits, and these may be the regions where InSAR works best.

[7] We considered InSAR result that was derived from a SAR data set acquired by the ENVISAT satellite. We have chosen these data because ENVISAT acquired multiple images from the same viewing geometry over Llaima

[1]Department of Physics of the Earth, Helmholtz-Centre Potsdam, Deutsches GeoForschungsZentrum, Potsdam, Germany.
[2]Now at Department of Earth and Planetary Science, University of California, Berkeley, California, USA.

0094-8276/11/2011GL047168

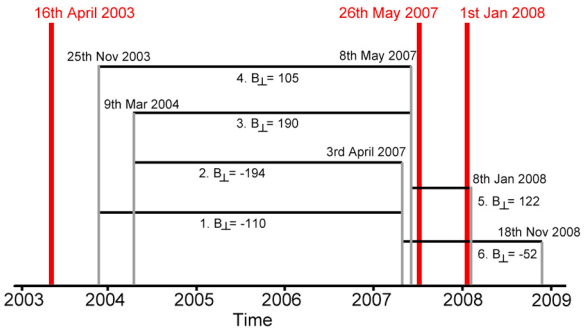

Figure 1. The timing of the eruptions are marked by the red lines and the generated interferograms are shown with the black lines with their according perpendicular baselines in [m]. The end points of the black lines are associated with the acquisition time of the master and slave images.

volcano before the year 2007. The data were acquired between 11/25/2003 and 11/18/2008 in descending orbit from track 10 in I2 mode.

[8] The interferometric processing of the radar data set was done using the freely available Roi_Pac processor provided by JPL [*Rosen et al.*, 2004]. The geometric phase was calculated and subtracted using satellite ephemeris data and a reference digital elevation model (DEM), obtained by shuttle radar thematic mapper (SRTM) at 90 m resolution. After estimating the phase coherence, each differential interferogram in Figure 2, was filtered using an adaptive filter coefficient of 0.5 [*Goldstein and Werner*, 1998]. The interferograms, after further investigation are shown in Figure 2, revealing several fringes at the volcano edifice, yet illustrating the prevalence of areas affected by significant phase decorrelation (hereafter referred to as noise).

[9] Significant noise is affecting the InSAR pixels close to the summit. The extent of snow and glaciers is well in agreement with the extent of noise at the elevated regions in the interferograms (see comparison of the InSAR data to Landsat data in Figure 2). Moreover, the areas of dense vegetation at the lower aprons and surroundings of Llaima volcano (reddish colors in Figure 2, left) are also affected by noise in the InSAR data. In contrast, InSAR provides reasonable data quality at regions where recent volcanic products have been emplaced.

[10] Therefore, comparison of the InSAR and Landsat data shows that the InSAR data are heavily affected by phase decorrelation due to vegetation, and snow cover. Furthermore, decorrelation due to topography is common at many other steep-sided strato-volcanoes elsewhere, and so the InSAR method could be deemed ineffective [*Pinel et al.*, 2011]. In the following section we outline how we applied a phase unwrapping and inverse modeling approach to obtain unambiguous displacement data with the aim of retrieving further information about the source of the deformation field at Llaima volcano.

3. Modeling Strategy

[11] Estimating the location and temporal change of a deformation source is one of the major tasks in volcano geodesy [*Dzurisin*, 2006]. The quality of source model parameters however, is strictly related to the quality and spatial distribution of the data sets [*Shirzaei and Walter*,

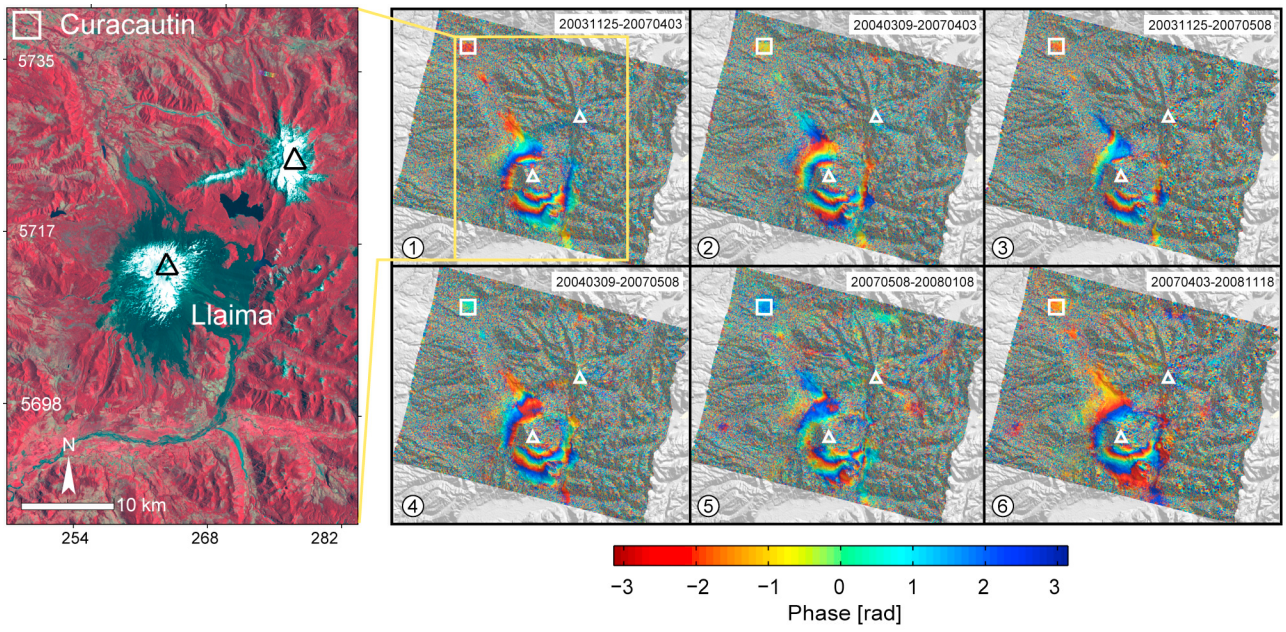

Figure 2. (left) Landsat TM image from 1987-01-15 at Llaima volcano in false color where the red, green and blue channels are the bands 4, 3 and 2, respectively. Red color in the image indicates vegetation, white color shows snow and dark grey colors indicate exposed rocky surfaces, here mainly historical lahars and pyroclastic flow deposits. (right) Selected interferograms at Llaima volcano. High coherence is shown only in those areas where no snow or vegetation is seen. Curacautin city (white rectangle) is at approximately 30 km distance from the Llaima summit. White triangles depict the summit craters of the active Llaima and the dormant Sierra Nevada stratovolcanoes.

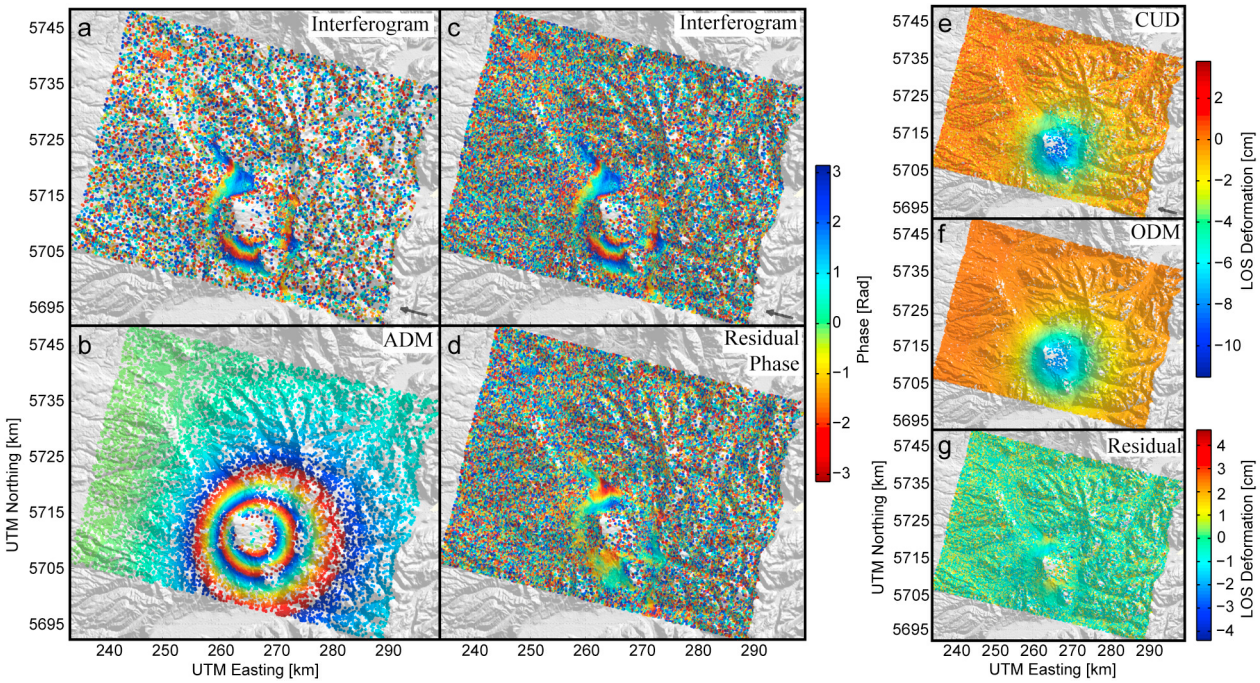

Figure 3. InSAR data and source modeling results at Llaima volcano, illustrated for one of six interferograms (here SAR scene pair 2003-11-25 and 2007-05-08). (a) Observed wrapped phase data with coherence threshold of 0.24. (b) Synthetic phase data from the approximate deformation model (ADM). (c) Observed wrapped phase data with coherence threshold of 0.17 from the same SAR scenes as Figure 3a. (d) Phase residual between observed wrapped phase data with low coherence (Figure 3c) and synthetic phase data from the ADM (Figure 3b). (e) Line of sight deformation (LOS) of the complete unwrapped data set (CUD). (f) Synthetic LOS deformation for the optimum deformation model (ODM) for the CUD (Figure 3e). (g) LOS deformation residual between the CUD (Figure 3e) and the synthetic LOS deformation for the ODM (Figure 3f).

2009]. The requirement for further InSAR data handling is that the phase difference between two neighboring data points is less than pi. Significant decorrelation reduces the spatial sampling (i.e., the number of pixels) and therefore introduces spatial aliasing errors. The aliasing error may be reduced by decreasing the amplitude of the phase changes throughout the interferogram [*Feigl and Thurber*, 2009]. This we performed by subtracting the phase contribution of an approximate deformation model (ADM) (e.g., Mogi-type source after [*Mogi*, 1958]) from the wrapped filtered data. In this way, although the sampling rate remains low, the phase difference between neighboring data points is less than pi over most of the data set, which allows the application of a reliable phase unwrapping.

[12] To obtain the ADM, we inverted the wrapped filtered data following *Feigl and Thurber*, [2009] by using the genetic algorithm (GA) presented in *Shirzaei and Walter*, [2009]. We adapted it in such a way that the modeled deformation ΔR_{mod} is converted to the modeled unambiguous phase $\psi_{mod} = \frac{-4\pi}{\lambda} \Delta R_{mod}$ [*Hanssen*, 2001]. By applying the modulus function $\phi_{mod} = \mathrm{mod}(\psi_{mod} + \pi, 2\pi)$, the modeled unambiguous phase ψ_{mod} was converted to a modeled wrapped phase ϕ_{mod}. The phase residual θ between the observed wrapped filtered phase ϕ_{obs} and the modeled wrapped phase ϕ_{mod} defined the cost in the GA and was minimized following L^1 - norm: $\theta = wrap(\phi_{obs} - \phi_{mod})$. For the wrapping operator we used the modulo function described above, i.e., $\theta = \mathrm{mod}(\phi_{obs} - \phi_{mod} + \pi, 2\pi) - \pi$.

[13] After subtracting the ADM, we used the minimum cost flow algorithm [*Chen and Zebker*, 2001], which is an L1- norm minimization approach [*Ahuja et al.*, 1993], for unwrapping the residual phase values θ. The complete unwrapped data set was obtained by restoring the ADM to the unwrapped residual phase values. Finally, we computed the source parameters of the deformation field by applying GA to the complete unwrapped data (CUD) set, by using a similar inversion approach as mentioned above.

4. Application to Llaima Volcano

[14] In this section we present the pair that spans the period 11/25/2003 – 05/08/2007; results summarizing the analysis of the other interferograms (Figure 2) are shown in the auxiliary material.[1] Let's consider only pixels with a phase coherence above 0.24, which provides us with about 25,000 useful data points (see interferogram in Figure 3a). The data shows a pronounced phase gradient approximately centered at the volcano. Moreover the area of phase decorrelation is visible on the base and the flanks. The ADM obtained by inverting this interferogram is given in Figure 3b. To calculate the residual phase (Figure 3d) we set a lower phase coherence threshold (0.17). This provided us with a larger group of pixels (Figure 3c) which may be more affected by phase noise. This step-wise increase in obser-

[1] Auxiliary materials are available in the HTML. doi:10.1029/2011GL047168.

Table 1. Inversion Results for a Mogi Source for the Interferograms Shown in Figure 1

Dates	Optimum Solution		Confidence Interval 95%	
	d [km]	ΔV [km^3]	d [km]	ΔV [km^3]
1. 20031125-20070403	6.8	−0.018	6.2–9.6	−0.021, −0.01
2. 20040309-20070403	9.9	−0.018	5.8–10.2	−0.023, −0.013
3. 20031125-20070508	9.9	−0.036	8.0–12.0	−0.043, −0.025
4. 20040309-20070508	9.7	−0.037	8.6–12.1	−0.045, −0.028
5. 20070508-20080108	6.2	0.012	5.3–9.3	0.006, 0.02
6. 20070403-20081118	5.1	0.007	4.1–8.3	0.006, 0.014

vation points did not lead to significant global unwrapping errors [*Marshall and Bethel*, 1996], since we used an L1 norm minimization approach for phase unwrapping [*Costantini*, 1998] and we reduced the spatial aliasing by removing the ADM. Hereafter we unwrapped the residual phase and restored the ADM, so that eventually the complete unwrapped data set was obtained (Figure 3e). As a test, we unwrapped the filtered interferograms without removing the ADM and noted significant unwrapping errors.

[15] As applied below for the Llaima data set, this set can be further used for final deformation source modeling. We initialized GA with a population size of 80, a selection rate of 0.5, a mutation rate of 0.6 and with 300 iterations (further details on implementation of GA are given by *Shirzaei and Walter* [2009]). The obtained model result is presented in the optimum deformation model (ODM) and the residual, can be explained as the subtraction of the true data from the model (Figures 3f and 3g). These results show that the implemented unwrapping and modeling strategy is capable of retrieving a complete spatial deformation field at Llaima and enables investigation of the deformation source parameters.

5. Results

[16] The unwrapped InSAR data set allows us to clearly identify and analyze two distinct periods of activity at Llaima volcano. A period of subsidence is sampled by the InSAR data acquired between 11/2003 and 05/2007. Then the InSAR data suggest a period of uplift, lasting at least until 11/2008. Given the available temporal sampling, the periods of subsidence and uplift are likely to be related to the eruptive episodes at Llaima. The period of subsidence occurred after the 04/2003 eruption, followed by uplift spanning the 05/2007 and 01/2008 eruptive episodes. We note that the sum of displacement estimated by adding both periods together is almost zero.

[17] The result of applying the modeling method to the data set is provided in Table 1. The source parameters and associated uncertainties are estimated at a confidence level of 95%. For both the subsidence and the uplift periods, the magma body location is at an approximately stable position of 262.95 km and 5711.25 km, according to the UTM projection system (zone H19). Therefore the location is shifted slightly (~1 km) to the southeast with respect to the summit crater of Llaima. The position of the subsidence source is constrained at a depth of 6 – 12 km, whilst the uplift source is located at a somewhat shallower depth of 4 – 9 km. Therefore, although being located at similar depths within the ranges of uncertainty, the inflation source appears to be somewhat shallower. The volumes of the deflation and inflation periods are between $4.5 – 10 \times 10^6$ m^3 and $6 – 20 \times 10^6$ m^3, respectively, and so the cumulative volume change at the location of the inferred magmatic source is minor over the entire observation period.

6. Discussion and Conclusion

[18] Detection of volcano deformation is one of the most important sources of information for monitoring programs, yet to date it has had limited success, particularly at steep-sided andesitic or basaltic-to-andesitic volcanoes. Detection of deformation occurrence, and especially localization and quantification of potential magma reservoirs at depth, and their behavior, is of major relevance because these volcanoes commonly typify the most explosive form of volcanism.

[19] This work presents an InSAR and modeling study at Llaima volcano. Using a SAR data set of the Envisat satellite in descending orbit (Figure 1), this work presents six interferograms. We note however, that a much larger SAR database is available. In total we processed 101 interferograms, but for most of the images phase decorrelation was too significant, as the two-pass interferometry could have allowed any interpretation. The application of standard-time series analysis was not feasible either, as it decreases the spatial coverage of the data significantly at steep-sided volcanoes, in such a way as to make it barely possible to observe the deformation signal related to magmatic activity [*Pinel et al.*, 2011]. So we focused on further investigating interferograms from 2-pass interferometry, because source inversions require a spatially dense data set [*Shirzaei and Walter*, 2009].

[20] We successfully adapted and applied a strategy that increases the accuracy of phase unwrapping. This work suggested the employment of a model-assisted unwrapping approach. Using this we found two episodes of subsidence and uplift at the volcano edifice, between 11/2003 and 05/2007 and 05/2007 till 11/2008, respectively. The poor temporal resolution may have been a drawback, as the apparent subsidence and uplift periods were temporally sampled only by a few interferograms each. Any short term variation below the sampling interval may have been missed using this dataset.

[21] During the inverse source modeling we considered an inflating point source [*Mogi*, 1958] buried in an elastic homogeneous half-space medium. This was only a rough approximation, where finite or more complex source geometries as well as surface topography and material heterogeneities were not considered. We note, furthermore, that some small and localized deformation might exist at the low-coherence areas at the volcano summit or flanks. This is not resolvable by our data and model. We nevertheless consider our use of such a simple model set-up to be a valid approach, because it allows us to explain the general pattern of the deformation signal. Moreover, use of a more complex model is hindered because very little is known about the deep-level mechanical properties and plumbing system geometry below Llaima. Furthermore, atmospheric delay in repeat pass interferometry [*Goldstein*, 1995] may have obscured the deformation data, which we did try to overcome by comparing inversion results from several interferograms spanning each period. MERIS data resolution is insufficient to accurately estimate the atmospheric delay for this small area.

[22] As a result of the inverse modeling procedure we found that the sources of subsidence and uplift are characterized by an absolute volume change rate of $3 – 13 \times 10^6$ m^3/yr and $9 – 30 \times 10^6$ m^3/yr, respectively. Thus in spite of the occurrence of two eruptions during the uplift period, the Llaima inflation rate is still ~3 times faster than the deflation rate, meaning that the magma supply to the reservoir is much faster than the magma withdrawal. This may mean that only relatively short pre-eruptive deformation precursors can be expected, making successful and timely monitoring and early warning strategies even more difficult.

[23] Following the inverse modeling, we inferred the deflating and inflating sources at the depths of 6 – 12 km and 4 – 9 km responsible for the subsidence and uplift periods, respectively. We hypothesize that the inflation and the deflation sources are actually imaging the same deep reservoir system. We note, however, that the variability of the source depths between the subsidence and the uplift period is similarly observed elsewhere and can be due to several reasons, including 1) the uncertainty of the data and depth estimation through inverse modeling [*Dawson and Tregoning*, 2007], 2) a more complexly shaped, possibly vertically distributed, source rather than a single-point source, 3) upward migration of the magma during the magma inflow into the reservoir, 4) combined magmatic and hydrothermal activity as observed for example at Campi Flegrei, Italy [*Battaglia et al.*, 2006].

[24] The depth-range provided gives, for the first time, a rough estimation of the Llaima magma plumbing system. Volcanoes throughout the Andes' Southern Volcanic Zone show evidence of sources at 3 to 9 km, e.g., at Cordon Caulle (4 – 7 km), Maule (5 – 9 km), Copahue (3 – 6 km) [*Fournier et al.*, 2010], hence they are at similar depth or somewhat shallower than at Llaima. More to the north, in the Andean Central Volcanic Zone, sources are at 5 –18 km, e.g., at Hualca Hualca (8 – 18 km), Cerro Blanco (5 – 10 km) [*Pritchard and Simons*, 2004], or Lazufre (8 – 13 km) [*Ruch et al.*, 2008], hence being somewhat deeper than at Llaima. Although these source depths are of great uncertainty, Llaima volcano appears to host a reservoir at a depth that is in line with volcanoes investigated in the same setting.

[25] **Acknowledgments.** This work was financially supported by the PROGRESS project and the project DFG WA1642/4-1. Data analyzed for this project was acquired by the European satellite ENVISAT and provided via the cat-1 proposal ID 3455. Discussions with Henriette Sudhaus and Eoghan Holohan are greatly appreciated. The authors thank two anonymous reviewers for their assistance in evaluating this paper.

[26] The Editor thanks two anonymous reviewers for their assistance in evaluating this paper.

References

Ahuja, R. K., T. L. Magnati, and J. B. Orlin (1993), *Network Flows*, Prentice-Hall, Theory, N. Y.

Battaglia, M., C. Troise, F. Obrizzo, F. Pingue, and G. De Natale (2006), Evidence for fluid migration as the source of deformation at Campi Flegrei caldera (Italy), *Geophys. Res. Lett.*, *33*, L01307, doi:10.1029/2005GL024904.

Chen, C. W., and H. A. Zebker (2001), Two-dimensional phase unwrapping with use of statistical models for cost functions in nonlinear optimization, *J. Opt. Soc. Am. A Opt. Image Sci. Vis.*, *18*, 338–351, doi:10.1364/JOSAA.18.000338.

Costantini, M. (1998), A novel phase unwrapping method based on network programming, *IEEE Trans. Geosci. Remote Sens.*, *36*(3), 813–821, doi:10.1109/36.673674.

Dawson, J., and P. Tregoning (2007), Uncertainty analysis of earthquake source parameters determined from InSAR: A simulation study, *J. Geophys. Res.*, *112*, B09406, doi:10.1029/2007JB005209.

Dzierma, Y., and H. Wehrmann (2010), Eruption time series statistically examined: Probabilities of future eruptions at Villarrica and Llaima volcanoes, Southern Volcanic Zone, Chile, *J. Volcanol. Geotherm. Res.*, *193*(1–2), 82–92, doi:10.1016/j.jvolgeores.2010.03.009.

Dzurisin, D. (2006), *Volcano Deformation: Geodetic Monitoring Techniques*, Springer, Berlin.

Feigl, K. L., and C. H. Thurber (2009), A method for modelling radar interferograms without phase unwrapping: application to the M 5 Fawnskin, California earthquake of 1992 December 4, *Geophys. J. Int.*, *176*(2), 491–504, doi:10.1111/j.1365-246X.2008.03881.x.

Fournier, T. J., M. E. Pritchard, and S. N. Riddick (2010), Duration, magnitude, and frequency of subaerial volcano deformation events: New results from Latin America using InSAR and a global synthesis, *Geochem. Geophys. Geosyst.*, *11*, Q01003, doi:10.1029/2009GC002558.

Galle, B., M. Johansson, C. Rivera, Y. Zhang, M. Kihlman, C. Kern, T. Lehmann, U. Platt, S. Arellano, and S. Hidalgo (2010), Network for Observation of Volcanic and Atmospheric Change (NOVAC)—A global network for volcanic gas monitoring: Network layout and instrument description, *J. Geophys. Res.*, *115*, D05304, doi:10.1029/2009JD011823.

Goldstein, R. M. (1995), Atmospheric limitations to repeat-track radar interferometry, *Geophys. Res. Lett.*, *22*(18), 2517–2520, doi:10.1029/95GL02475.

Goldstein, R. M., and C. L. Werner (1998), Radar interferogram filtering for geophysical applications, *Geophys. Res. Lett.*, *25*(21), 4035–4038, doi:10.1029/1998GL900033.

Hanssen, R. F. (2001), *Radar Interferometry*, Kluwer Acad., Dordrecht, Netherlands.

Marshall, J., and J. Bethel (1996), Basic concepts of L1 norm minimization for surveying applications, *J. Surv. Eng.*, *122*, 168–179, doi:10.1061/(ASCE)0733-9453(1996)122:4(168).

Mogi, K. (1958), Relations between the eruptions of various volcanoes and the deformation of the ground surfaces around them, *Bull. Earthquake Res. Inst. Univ. Tokyo*, *36*, 99–134.

Naranjo, J. A., and H. Moreno (1991), Actividad explosiva postglacial en el volcan Llaima, Andes del sur (38°45 ′S), *Rev. Geol. Chile*, *18*(1), 69–80.

Pinel, V., A. Hooper, S. De la Cruz-Reyna, G. Reyes-Davila, M. P. Doin, and P. Bascou (2011), The challenging retrieval of the displacement field from InSAR data for andesitic stratovolcanoes: Case study of Popocatepetl and Colima Volcano, Mexico, *J. Volcanol. Geotherm. Res.*, *200*(1–2), 49–61, doi:10.1016/j.jvolgeores.2010.12.002.

Pritchard, M. E., and M. Simons (2004), An InSAR-based survey of volcanic deformation in the central Andes, *Geochem. Geophys. Geosyst.*, *5*, Q02002, doi:10.1029/2003GC000610.

Rosen, P. A., S. Henley, G. Peltzer, and M. Simons (2004), Updated repeat orbit interferometry package released, *Eos Trans. AGU*, *85*(5), doi:10.1029/2004EO050004.

Ruch, J., J. Anderssohn, T. R. Walter, and M. Motagh (2008), Caldera-scale inflation of the Lazufre volcanic area, South America: Evidence from InSAR, *J. Volcanol. Geotherm. Res.*, *174*, 337–344, doi:10.1016/j.jvolgeores.2008.03.009.

Shirzaei, M., and T. R. Walter (2009), Randomly iterated search and statistical competency as powerful inversion tools for deformation source modeling: Application to volcano interferometric synthetic aperture radar data, *J. Geophys. Res.*, *114*, B10401, doi:10.1029/2008JB006071.

Siebert, L., and T. Simkin (2002), Volcanoes of the world: An illustrated catalog of Holocene volcanoes and their eruptions, *Global Volcanism Program Digital Inf. Ser. GVP-3*, Smithsonian Inst., Washington, D. C. [Available at http://www.volcano.si.edu/world/.]

H. Bathke, M. Shirzaei, and T. R. Walter, Department of Physics of the Earth, Helmholtz-Centre Potsdam, Deutsches GeoForschungsZentrum, Telegrafenberg, D-14473 Potsdam, Germany. (bathke@gfz-potsdam.de)